Current Measurements by SAR Along-Track Interferometry From a Space Shuttle

Roland Romeiser, *Member, IEEE*, Helko Breit, Michael Eineder, *Member, IEEE*, Hartmut Runge, Pierre Flament, *Member, IEEE*, Karin de Jong, and Jur Vogelzang

***Abstract*—We present one of the first studies on ocean current retrievals from interferometric synthetic aperture radar (InSAR) data acquired during the Shuttle Radar Topography Mission (SRTM) in February 2000. The InSAR system of SRTM was designed for high-resolution topographic mapping of the Earth's land surfaces, using two SAR antennas on a Space Shuttle with a cross-track separation of 60 m. An additional along-track antenna separation of 7 m resulted in an effective time lag of about 0.5 ms between the two images, which could theoretically be exploited for target velocity retrievals. However, the feasibility of ocean current measurements with SRTM has been questionable, since the time lag was much shorter than the theoretical optimum (about 3 ms at X-band) and the signal-to-noise ratio over water was quite low. Nevertheless, some X-band InSAR images of coastal areas exhibit clear signatures of tidal flow patterns. As an example, we discuss an image of the Dutch Wadden Sea. We convert the InSAR data into a line-of-sight current field, which is then compared with results of the numerical circulation model KUSTWAD. For tidal phases close to the conditions at the time of the SRTM overpass; we obtain correlation coefficients of up to 0.6 and rms differences on the order of 0.2 m/s. Furthermore we find that SRTM resolves current variations down to spatial scales on the order of 1 km. This is consistent with predictions of a numerical InSAR imaging model. Remaining differences between SRTM- and KUSTWAD-derived currents can be attributed mainly to residual motion errors in the SRTM data as well as to a limited representation of the conditions at the time of the SRTM overpass in the available KUSTWAD results.**

***Index Terms*—Current measurements, interferometric synthetic aperture radar (InSAR), Shuttle Radar Topography Mission (SRTM).**

I. Introduction

THE fundamental principles of current measurements by along-track interferometric synthetic aperture radar (InSAR) have been known since the 1980s [1]. The along-track InSAR combines the high spatial resolution of a conventional SAR on the order of meters with the capability to measure line-of-sight (LOS) target velocities. This is achieved by using two SAR antennas which are separated by some distance in flight direction and acquire two images of the same scene with a time lag on the order of milliseconds. Conventional SAR processing exploits the Doppler history of each individual received signal for the synthetization of a long antenna and a corresponding improvement of the azimuthal resolution of the image; the resulting image does not contain explicit information on target velocities. However, an interferometric combination of two complex SAR images acquired with a short time lag reveals phase differences which are proportional to the mean Doppler offset of the backscattered signal mapped into each individual pixel and thus to the LOS velocity of the scatterers. Since the late 1980s, current measurements by airborne along-track InSAR have been demonstrated in several experiments [2]–[4], and various authors have presented theoretical models for the contributions of surface currents and wave motions to the detected velocities [5], [6] as well as studies on the potential of spaceborne InSARs for oceanic applications and favorable system parameters [7]. Until now, there has been no (civilian) satellite with an operational along-track InSAR. However, we will show in this paper that InSAR data from the Shuttle Radar Topography Mission (SRTM) in February 2000 are suitable for a first demonstration of current measurements from space.

The main objective of SRTM was the generation of high-resolution, high-precision topographic maps of the Earth's land surfaces with a single-pass, dual-frequency (C- and X-band) cross-track InSAR on the Space Shuttle *Endeavour* [8]. The cross-track InSAR technique requires an antenna separation by some distance perpendicular to the flight direction. In this case the detected phase differences are proportional to topographic elevations from a reference plane [9], [10]. The physical cross-track antenna separation of SRTM was 60 m, which corresponds to an effective cross-track baseline of 30 m between the phase center of the transmitting and receiving primary antenna in the cargo bay of the Space Shuttle and the phase center formed half-way between the primary antenna and the receive-only secondary antenna at the end of an expanded mast structure. This translates into a height sensitivity of approx. 175 m per phase cycle of 2π at X-band (9.6 GHz) and an incidence angle of 55°. For technical reasons, the canister containing the mast had to be mounted ahead of the primary antenna in the cargo bay, which created an additional along-track antenna separation of 7 m (or effective along-track baseline of 3.5 m). An artist's view of the SRTM configuration in space is shown in Fig. 1. System parameters of SRTM which are relevant to this work are summarized in Table I.

Manuscript received February 21, 2005; revised July 6, 2005. This work was supported in part by the German Aerospace Center (DLR), Bonn, Germany, under Contract 50 EE 0100 and in part by the European Space Agency (ESA-ESTEC), Noordwijk, Netherlands, under Contract 16100/02/NL/EC.

R. Romeiser is with the Institut für Meereskunde, Zentrum für Meeres- und Klimaforschung, Universität Hamburg, 20146 Hamburg, Germany (e-mail: romeiser@ifm.uni-hamburg.de).

H. Breit, M. Eineder, and H. Runge are with the Institut für die Methodik der Fernerkundung, Deutsches Zentrum für Luft- und Raumfahrt, 82234 Wessling, Germany.

P. Flament is with the School of Ocean and Earth Science and Technology, University of Hawaii, Honolulu, HI 96817 USA.

K. de Jong is with the Rijksinstituut voor Kust en Zee, Rijkswaterstaat, 2518 AX The Hague, The Netherlands.

J. Vogelzang was with the Adviesdienst voor Geo-informatie en ICT, Rijkswaterstaat, 2622 HA Delft, The Netherlands. He is now at Koninklijk Nederlands Meteorologisch Instituut, 3732 GK, De Bilt, The Netherlands.

Digital Object Identifier 10.1109/TGRS.2005.856116

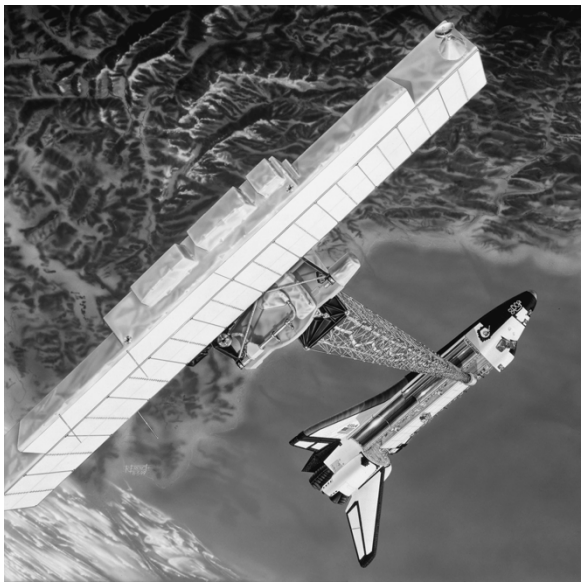

Fig. 1. Artist's view of the SRTM configuration in space. Note that the mast with the outboard antennas is installed ahead of the main antennas in the cargo bay, which leads to an along-track separation of 7 m between the phase centers of the main antennas and the outboard antennas. Courtesy of Ball Aerospace & Technologies Corp.

TABLE I
SRTM/X-SAR SYSTEM PARAMETERS

Radar Frequency	9.6 GHz
Polarization	VV
Incidence Angle	55°
Cross-Track Antenna Separation	60 m
Along-Track Antenna Separation	7 m
Height Sensitivity	175 m / 2π
Horizontal Velocity Sensitivity	38.5 m/s / 2π
Instrument Noise Level	–29 dB
Orbit Altitude	233 km
Orbit Velocity	7500 m/s
Heading (Wadden Sea)	56°
Look Direction (Wadden Sea)	326°

The along-track separation between the antennas resulted in a time lag of about 0.5 ms between the two InSAR images. One can show that a combined cross-track/along-track InSAR with antenna separations in both directions works effectively as a pure cross-track InSAR over land (where there are almost no moving targets) and as a pure along-track InSAR over water (where there are almost no height variations on the resolved spatial scales) [7]. However, the feasibility of current measurements with SRTM has not been obvious, since the time lag of 0.5 ms is quite short and yields a poor sensitivity to small current variations: At X-band, a phase cycle of 2π corresponds to a horizontal LOS velocity range of as much as 38.5 m/s, i.e., a relatively large surface current difference of 1 m/s between two locations in an image translates into a phase difference of less than 10°. Ideal time lags for ocean current measurements by X-band InSAR would be on the order of about 2–5 ms, where the lower limit is determined by the condition that phase variations associated with the target velocities of interest should be larger than the instrument noise contributions and the upper limit is determined by the temporal decorrelation of the backscattered signal and the occurrence of phase wrapping problems [6], [7]. Furthermore, the relatively high incidence angle of 55° in combination with an instrument noise level of about −29 dB leads to low signal-to-noise ratios over calm waters at low wind speeds. Finally, the amount of data acquired over water is very limited. Nevertheless, some phase images of coastal areas appear to exhibit clear signatures of tidal flow patterns. We have analyzed one of those images.

The paper is structured as follows. In Section II we present an amplitude and phase image of the western Wadden Sea off the Dutch coast and discuss their basic properties. A procedure for correcting and filtering the phase image and converting it into a LOS surface current field is then described in Section III. In Section IV we give an overview of the numerical circulation model KUSTWAD, whose output current fields for different tidal phases are then compared with the SRTM result in Section V. In Section VI we discuss relations between the actual SRTM-derived current field and a corresponding theoretical data product obtained from the numerical InSAR imaging model M4S. Finally, conclusions are drawn in Section VII.

II. SRTM IMAGE OF THE DUTCH WADDEN SEA

On February 15, 2000, 12:34 UTC, SRTM acquired an X-band InSAR image of the western Wadden Sea between the Dutch mainland, the dam ("Afsluitdijk") that separates Lake IJssel from the Wadden Sea, and the islands Texel, Vlieland, and Terschelling. The data were processed to a SAR interferogram and to a digital elevation model at DLR Oberpfaffenhofen, Germany. The operational InSAR processing comprises SAR focusing with motion compensation, coregistration of the two SAR images on subpixel level, interferogram generation, phase unwrapping and removal of the phase pattern corresponding to a stationary reference ellipsoid, and, finally, phase to height conversion [11]. The standard data product obtained this way was provided to the University of Hamburg for analysis. The original amplitude and phase images are shown in Fig. 2, where the pixel resolution of the amplitude image [Fig. 2(a)], which was obtained from DLR as a JPEG image at the shown quality level, is about 200 m × 200 m, and the pixel resolution of the phase image [Fig. 2(b)] has been reduced from 25 m × 25 m of the original dataset to 100 m × 100 m by averaging. The color-coded phase range is 0.72 rad, which corresponds to a topographic height interval of 20 m for cross-track InSAR contributions and a velocity interval of 4.4 m/s for along-track InSAR contributions.

III. DATA PROCESSING AND INTERPRETATION

The homogeneous brightness and texture of the SRTM amplitude image in the Wadden Sea indicates that most of this area, large parts of which can fall dry at low tides, was covered with water at the time of the SRTM overpass. While the amplitude image does not contain much more information, the phase signatures of the water surface exhibit pronounced spatial variations, which can be interpreted as signatures of height variations by as much as 10 m or signatures of LOS current variations by about 2 m/s. The latter interpretation appears much more realistic, but some large-scale phase variations which become visible as a region of relatively low phases (blue) northwest of Texel and a region of relatively high phases (red) along the

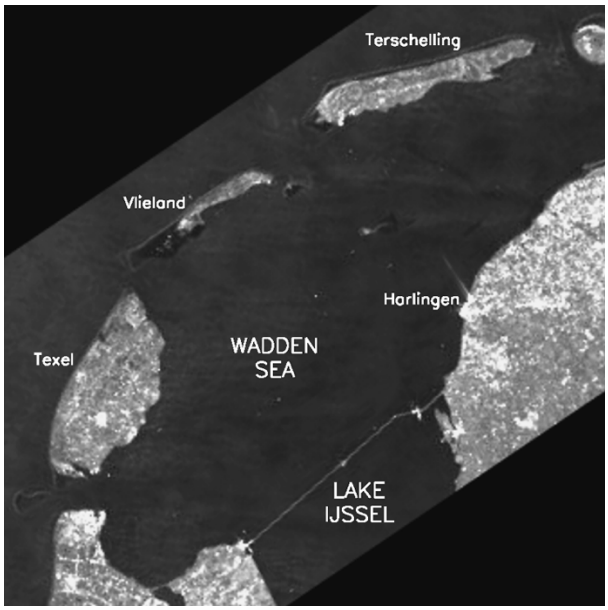

(a)

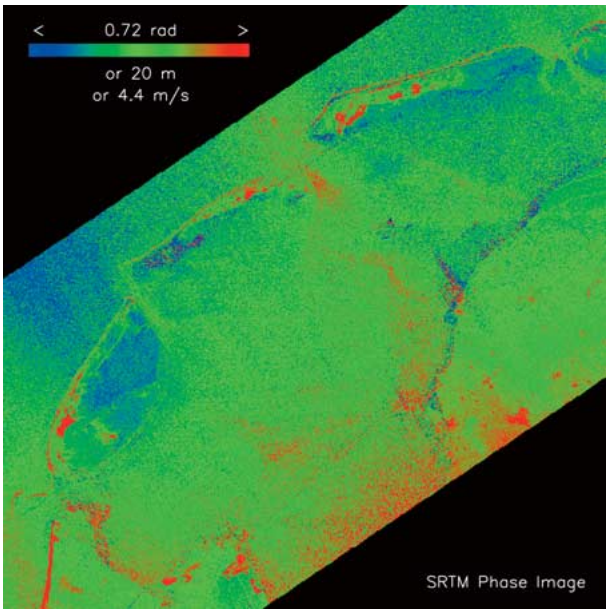

(b)

Fig. 2. X-band (a) amplitude image and (b) phase image of the western Dutch Wadden Sea [shown area size = 70 km × 70 km); (a) pixel size = 200 m × 200 m. (b) 100 m × 100 m] acquired by SRTM on February 15, 2000, 12:34 UTC. The radar look direction is toward northwest; the platform heading is toward northeast; and north is at the top of the images.

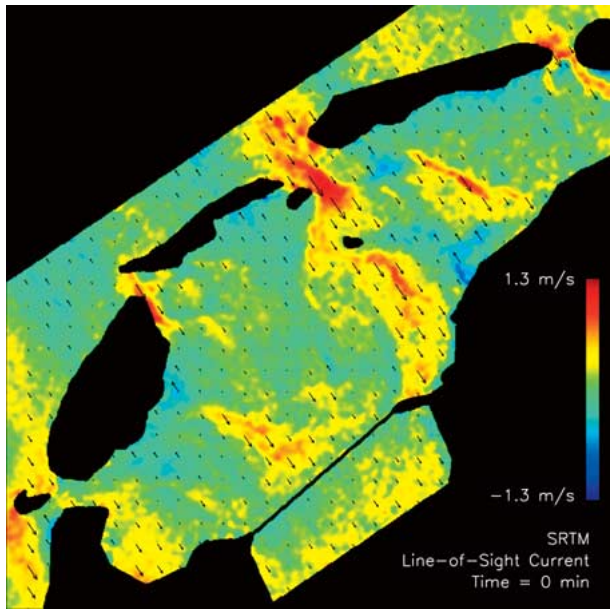

Fig. 3. Line-of-sight current field derived from the SRTM phase image of Fig. 2(b). Arrows indicate the orientation and strength of the current component parallel to the radar look direction.

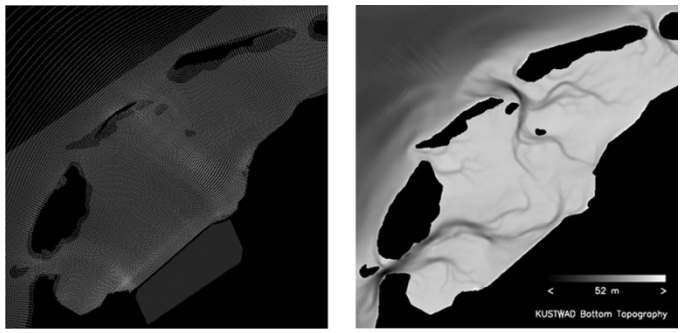

(a) (b)

Fig. 4. (a) KUSTWAD model grid points and SRTM swath and land mask and (b) KUSTWAD bottom topography in the 70 km × 70 km test area.

southeast (near-range) boundary of the swath may reflect topography artifacts resulting from shortcomings of the "flat" reference ellipsoid surface used in the interferometric processing or from cross-track baseline variations with oscillations of the antenna mast of the SRTM system (cf. Section VI).

For further processing of the data, we generated a land mask on the basis of the visible land/water boundaries in the amplitude image and maps of the area. Then phase variations at wavelengths of 20 km and longer were eliminated by highpass filtering. Finally, the data (at 100 m × 100 m pixel size) were low-pass filtered (smoothed) by running a 5 × 5 pixel running boxcar average filter three times and converted into horizontal LOS velocities. Except for an unknown mean offset, the averaging of the original data over 4 × 4 pixels and the smoothing narrows the confidence interval of each individual phase or velocity value (associated with statistical fluctuations) by a factor of about 1/35. In contrast to the airborne along-track InSAR data described in [4], which could be corrected for theoretical contributions of wave motions to obtain meaningful absolute LOS currents, the SRTM phase images are not absolutely calibrated, i.e., they include a quasi-arbitrary mean offset which may be adjusted on the basis of plausibility considerations. We decided to subtract a constant value such that a LOS velocity of 0 was obtained in the vicinity of the dam between Wadden Sea and Lake IJssel, where the radar look direction is almost perpendicular to the dam. Further corrections for spatially varying contributions of wave motions (cf. [4]) were not applied, since such corrections would be small compared to the remaining noise in the data on the resolved spatial scales and difficult to compute.

The resulting SRTM-derived LOS current field is shown in Fig. 3. It indicates a strong tidal flow into the Wadden Sea area with maximum currents between the islands on the order of

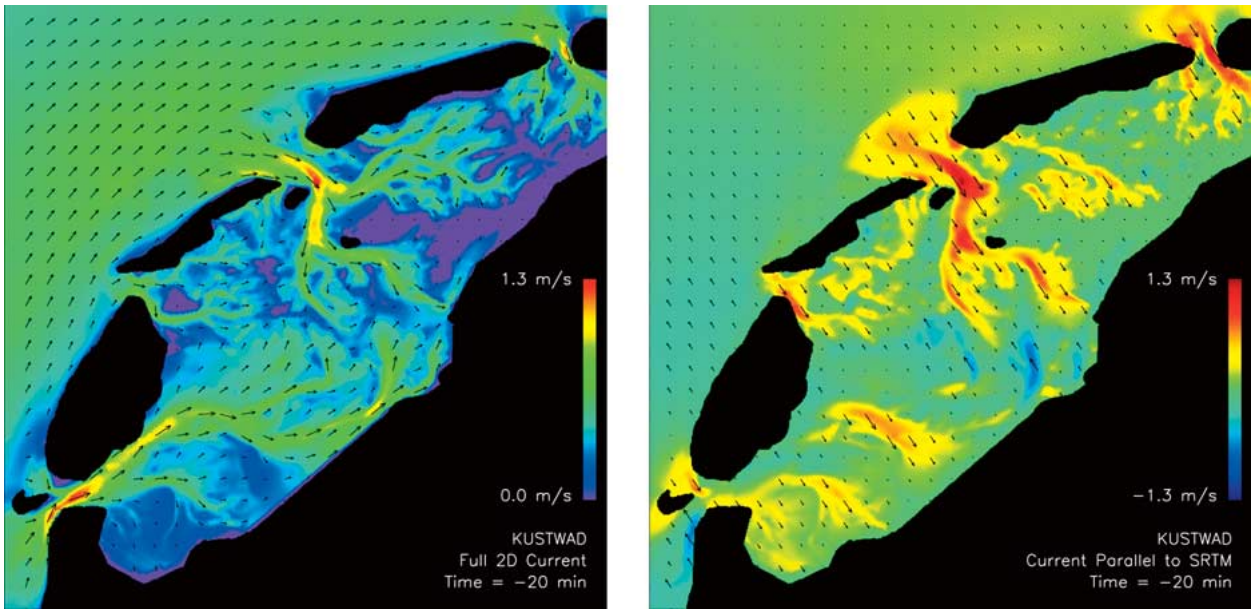

(a) (b)

Fig. 5. Full 2-D current field in the test area from KUSTWAD for (a) the tidal phase 20 min before the SRTM overpass and (b) component parallel to the look direction of SRTM. Interpolated onto the same 100 m × 100 m grid as the SRTM data of Figs. (2b) and 3.

1.2 m/s. The SRTM overpass took place 3:16 h before high water in West-Terschelling; the observed flow pattern is very similar (qualitatively and quantitatively) to the typical flow pattern at this tidal phase as shown in a current atlas [12]. For a full quantitative evaluation, scientists at the Dutch Directorate General of Public Works and Water Management (Rijkswaterstaat) were asked for reference data.

IV. Reference Currents From the KUSTWAD Model

KUSTWAD is one of the so-called WAQUA/TRIWAQ based hydraulic models [13] that are being developed and maintained at the National Institute for Coastal and Marine Management ("RIKZ" in Dutch) of Rijkswaterstaat in The Hague. Various versions of these models are available for simulations on different spatial scales, ranging from the Dutch Continental Shelf Model DCSM to more detailed local models such as KUSTWAD. They are employed in operational, management, and research activities. To calibrate the models and to improve the quality of the operational results, they have been extended with data assimilation modules [14], [15]. Both the two-dimensional (2-D) hydraulic model WAQUA and the three-dimensional (3-D) model TRIWAQ are based on advanced numerical methods. They include important physical processes such as salinity variations and turbulence, and they contain special features to model sluices, barriers, tidal flats, etc. These qualities are particularly important in areas such as the Wadden Sea.

KUSTWAD is specially developed to describe and predict the consequences of management measures in the Wadden Sea. The model contains the main part of the Dutch Wadden Sea, Lake IJssel, a part of the North Sea, and a part of the river IJssel. It has a curvilinear schematization with a resolution varying from 50 m up to 2.5 km. The representation of the bottom is based on the latest available depth data. Bathymetric surveys and the corresponding updates of depth maps of the Wadden Sea are carried out continuously according to a well defined scheme; a complete update for the whole area is obtained every six years at least. The model grid in the Wadden Sea (with SRTM swath and land mask) and the bottom topography used for the simulations discussed in the following are shown in Fig. 4.

To save time and costs, we have used existing KUSTWAD results instead of conducting dedicated simulations for the specific scenario of the SRTM overpass. The available off-the-shelf model results represent current fields in the uppermost layer of the 3-D version of KUSTWAD for one tidal cycle on March 23, 1995, 1:00 through 14:00 UTC (i.e., about five years before the SRTM overpass), with a time step of 1 h. Although the bottom topography may have changed during this period and other boundary conditions (e.g., the wind) may have been different in the two scenarios, one can expect some similarities of flow patterns and current strengths in the measured and simulated surface current fields for the same tidal phase. The shortest time lag between the tidal phase at the time of the SRTM overpass and an available KUSTWAD current field is 20 min. The full 2-D KUSTWAD current field for this tidal phase as well as its component parallel to the look direction of SRTM are shown in Fig. 5. For this visualization and all quantitative analyses, the KUSTWAD currents were interpolated onto the same 100 m × 100 m grid as the SRTM phases and LOS currents of Figs. 2(b) and 3, respectively.

V. Intercomparison of SRTM- and KUSTWAD-Derived Current Fields

The comparison of the SRTM-derived current field with KUSTWAD results has been carried out visually and statistically, where the statistical analysis comprises the computation of overall statistical parameters such as correlation and regression coefficients as well as parameters describing the agreement of spatial variations in the two datasets on different length scales. Since neither the InSAR data nor the circulation model results for March 1995 can be considered as "true" reference currents for the scenario at the time of the SRTM

overpass, the analysis has been symmetrized as much as possible. Furthermore we have considered KUSTWAD current fields for the whole tidal cycle, not only for the phase that theoretically corresponds best to the SRTM overpass.

A. Visual Intercomparison of the Current Fields

A look at the current fields of Fig. 3 and Fig. 5(b) indicates quite good qualitative and quantitative agreement: The current patterns, which exhibit a strong correlation with the bottom topography in the test area [cf. Fig. 4(b)], are very similar in the SRTM and KUSTWAD results, and also the magnitudes of the LOS currents are comparable. Similarly good agreement is found between the SRTM-derived current field and the KUSTWAD-derived current fields for the following time step (40 min after the tidal phases of the SRTM overpass, not shown), while the earlier and later KUSTWAD currents exhibit more pronounced differences from the SRTM result.

Fig. 5(a) indicates that the magnitudes of the 2-D KUSTWAD currents at the best fit tidal phase are zero in many grid points, which may indicate that these areas have fallen dry at this time in the simulation. Such grid points with no current according to KUSTWAD and a nonzero current according to SRTM have been excluded from the following statistical analyses.

B. Overall Statistical Analysis

For the overall statistical analysis, some fundamental statistical quantities that describe the relation between the LOS current field from KUSTWAD at time t with respect to the tidal phase of the SRTM overpass, $\boldsymbol{a}(t) = (a_{i,j})(t)$, and the LOS currents from SRTM $\boldsymbol{b}(0) = (b_{i,j})(t = 0)$ have been computed: the mean differences

$$\delta(t) = \langle b(0) - a(t) \rangle \tag{1}$$

the rms difference

$$\sigma(t) = \sqrt{\left\langle (b(0) - a(t))^2 \right\rangle} \tag{2}$$

the correlation coefficient

$$r(t) = \frac{\langle (a(t) - \langle a(t) \rangle)\,(b(0) - \langle b(0) \rangle) \rangle}{\sqrt{\left\langle (a(t) - \langle a(t) \rangle)^2 \right\rangle \left\langle (b(0) - \langle b(0) \rangle)^2 \right\rangle}} \tag{3}$$

and the symmetrical regression coefficient

$$c(t) = \operatorname{sgn}(r(t)) \sqrt{\frac{\left\langle (b(0) - \langle b(0) \rangle)^2 \right\rangle}{\left\langle (a(t) - \langle a(t) \rangle)^2 \right\rangle}} \tag{4}$$

where $\langle \ldots \rangle$ denotes spatial averaging over all valid data points. The symmetrical regression coefficient c is defined such that there is no preference for a minimization of rms differences between the regression line and the values of b, assuming that the values of a represent the reference, or vice versa. In principle, the conventional regression coefficients can be computed from our r and c values as $c \cdot |r|$ (minimization of the error of b) or $c/|r|$ (minimization of the error of a).

Fig. 6 shows scatter diagrams of the LOS currents from KUSTWAD at two tidal phases [20 min and 6 h 20 min (380 min) before the SRTM overpass] versus the ones from SRTM,

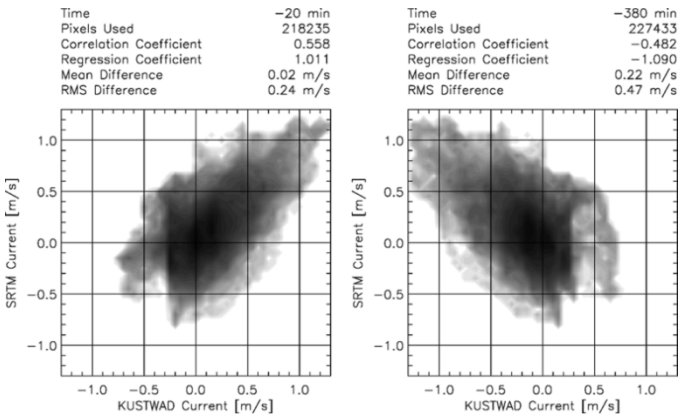

Fig. 6. Scatter diagrams showing the distribution of SRTM-derived versus KUSTWAD-derived currents and corresponding statistical quantities for tidal phases (in KUSTWAD) (a) 20 min and (b) 380 min before the SRTM overpass.

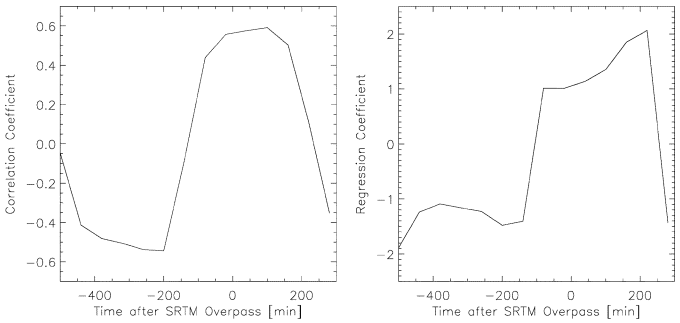

Fig. 7. (a) Correlation coefficient and (b) symmetrical regression coefficient between LOS current fields from KUSTWAD for the whole tidal cycle and the SRTM-derived current field.

as well as the corresponding statistical quantities. As expected, there is a positive correlation in one case and a negative correlation in the other case, where the KUSTWAD currents represent the opposite tidal phase. Note the small mean difference of only 0.02 m/s at −20 min [Fig. 6(a)], which indicates that our adjustment of the offset of the SRTM current field on the basis of values near the "Afsluitdijk" dam was quite successful. Also the symmetrical regression coefficient of 1.011 is a very good result. However, a correlation coefficient of 0.558 cannot be considered as a very good result; this will be examined in more detail in Section VI.

Fig. 7 shows all correlation coefficients and symmetrical regression coefficients for the whole tidal cycle in KUSTWAD. The diagrams depict that the best agreement between KUSTWAD and SRTM is obtained during the period from 80 min before through 160 min after the SRTM overpass. The maximum of the correlation is on the order of 0.6 (100 min after the overpass); the symmetrical regression coefficient is very close to 1 at −80 and −20 min. Also the best values of the mean difference (0.00 m/s) and of the rms difference (about 0.2 m/s) are found at 100 min (diagrams not shown). These results indicate that there may be a small phase shift in the KUSTWAD results, but in view of the fact that the KUSTWAD current fields are supposed to represent a scenario five years before the SRTM overpass, this small effect should not be overinterpreted.

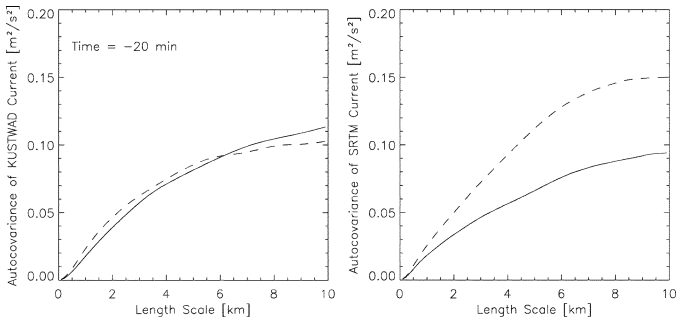

(a) (b)

Fig. 8. Autocovariance of (a) KUSTWAD- and (b) SRTM-derived LOS currents versus (solid lines) spatial displacement parallel and (dashed lines) perpendicular to the look direction of SRTM. The KUSTWAD result corresponds to the tidal phase 20 min before the SRTM overpass.

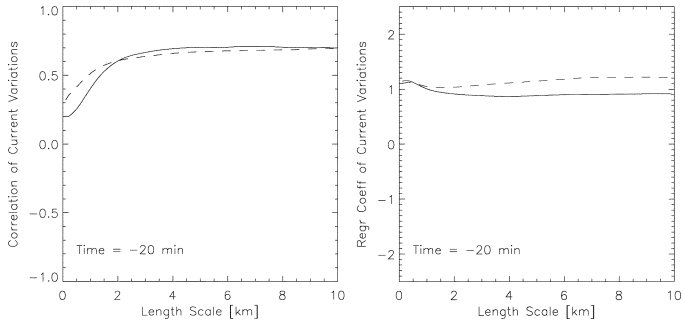

(a) (b)

Fig. 9. (a) Correlation coefficient and (b) symmetrical regression coefficient of variations in the SRTM and KUSTWAD currents versus (solid lines) spatial displacement parallel and (dashed lines) perpendicular to the look direction of SRTM. The KUSTWAD result corresponds to the tidal phase 20 min before SRTM overpass.

C. Analysis on Spatial Resolutions

Despite the low-pass filtering, the SRTM-derived current field appears to be more noisy than the KUSTWAD results. Furthermore, the filtering must have resulted in a reduced effective spatial resolution far below our grid cell size of 100 m × 100 m. In order to get an impression of the actual spatial resolution of the SRTM-derived currents, the following more detailed analysis has been carried out.

First, autocovariance matrices of the KUSTWAD- and SRTM-derived LOS current fields were computed. The 2-D autocovariance matrix $\boldsymbol{\sigma}^2$ of an array $\boldsymbol{a} = (a_{i,j})$ is defined by

$$\sigma^2_{m,n} = \left\langle (a_{i,j} - a_{i-m,j-n})^2 \right\rangle \tag{5}$$

It is a measure of the variance within $\boldsymbol{a}$ as function of the spatial length scale and direction. Results for variations in the look direction and the (perpendicular) flight direction of SRTM in the KUSTWAD current field for the tidal phase 20 min before the SRTM overpass and in the SRTM-derived current field (with indexes m, n converted into actual lengths) are shown in Fig. 8. While the autocovariance of the KUSTWAD LOS currents [Fig. 8(a)] is almost independent of the direction, the result for the SRTM data [Fig. 8(b)] indicates clearly larger variations in flight direction than in look direction. This difference may result from artifacts of the SAR image acquisition and processing techniques and algorithms (cf. Section VI) or from systematic shortcomings of the KUSTWAD model, but it may as well be an effect of different wind and wave scenarios or of spatial variations in the wind and wave field which have not been taken into account in the data processing. However, while the variations in flight direction are larger in the SRTM currents than in the KUSTWAD currents, the variations in look direction are smaller—the overall spatial variabilities in both datasets are comparable. Furthermore, the diagrams show that there is very little variability on length scales below 1 km in both datasets.

Fig. 9 shows correlation coefficients and symmetrical regression coefficients of the variations in the SRTM and KUSTWAD currents on different spatial scales parallel to the look and flight directions of SRTM. In this case the matrices of correlation and regression coefficients have been defined by (6) and (7), shown at the bottom of the page, respectively. Down to spatial scales on the order of 1 km (a little shorter in flight direction and longer in look direction), the correlation is larger than 0.5, while the symmetrical regression coefficient is close to 1 on all scales (however, an overestimation or underestimation of variations of the LOS current in flight direction by SRTM or by KUSTWAD, respectively, becomes visible once more in this diagram). This indicates that SRTM can basically detect and resolve all spatial variations of the LOS current which are relevant to the KUSTWAD model, down to scales on the order of 1 km, with constant accuracy.

VI. Intercomparison of Actual and Simulated SRTM-Derived Current Fields

For a further evaluation of the SRTM-derived current field and a test of the numerical InSAR imaging model M4S of the University of Hamburg [6], [7], a theoretical SRTM phase image of the Wadden Sea scenario was computed and processed with the same algorithm as the actual SRTM data to derive a theoretical SRTM-derived LOS current field. For the simulation, the 2-D KUSTWAD current field for the tidal phase 20 min before the SRTM overpass (Fig. 5) was used as model input. Based on weather observations in the test area, a wind speed of 5 m/s from west was assumed. Hydrodynamic wave–current interaction effects were neglected, but the surface wave spectrum at each grid

$$r_{m,n} = \frac{\left\langle \left(a_{i,j} - a_{i-m,j-n} - \langle a_{i,j} - a_{i-m,j-n}\rangle\right)\left(b_{i,j} - b_{i-m,j-n} - \langle b_{i,j} - b_{i-m,j-n}\rangle\right)\right\rangle}{\sqrt{\left\langle \left(a_{i,j} - a_{i-m,j-n} - \langle a_{i,j} - a_{i-m,j-n}\rangle\right)^2\right\rangle \left\langle \left(b_{i,j} - b_{i-m,j-n} - \langle b_{i,j} - b_{i-m,j-n}\rangle\right)^2\right\rangle}} \tag{6}$$

$$c_{m,n} = \operatorname{sgn}(r)\sqrt{\frac{\left\langle \left(b_{i,j} - b_{i-m,j-n} - \langle b_{i,j} - b_{i-m,j-n}\rangle\right)^2\right\rangle}{\left\langle \left(a_{i,j} - a_{i-m,j-n} - \langle a_{i,j} - a_{i-m,j-n}\rangle\right)^2\right\rangle}} \tag{7}$$

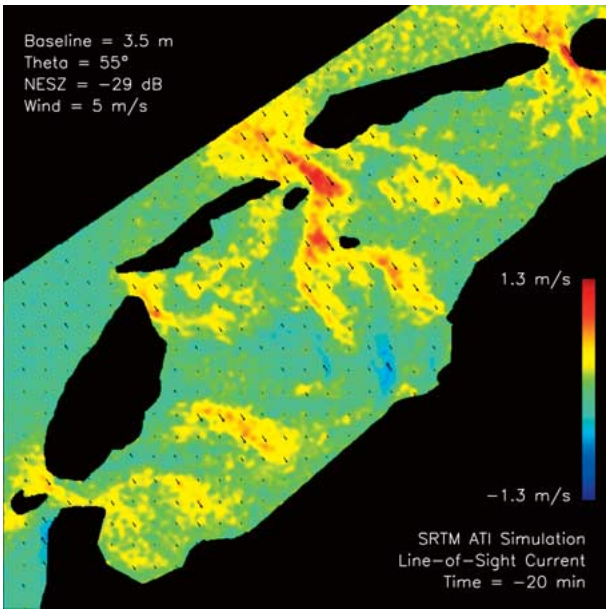

Fig. 10. Simulated SRTM-derived LOS current field obtained from the KUSTWAD current field for the tidal phase 20 min before the SRTM overpass (Fig. 5). Only grid points covered by the KUSTWAD model and by the swath of SRTM have been taken into account.

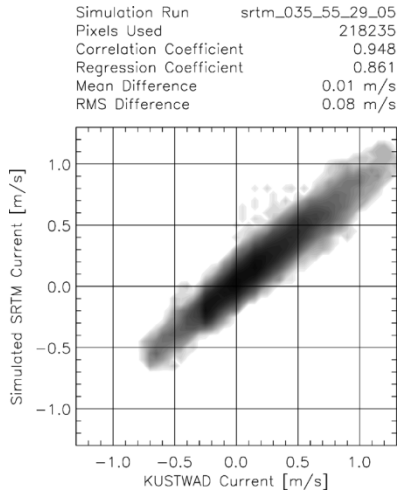

Fig. 11. Same as Fig. 6(a), but for simulated SRTM-derived currents versus KUSTWAD currents.

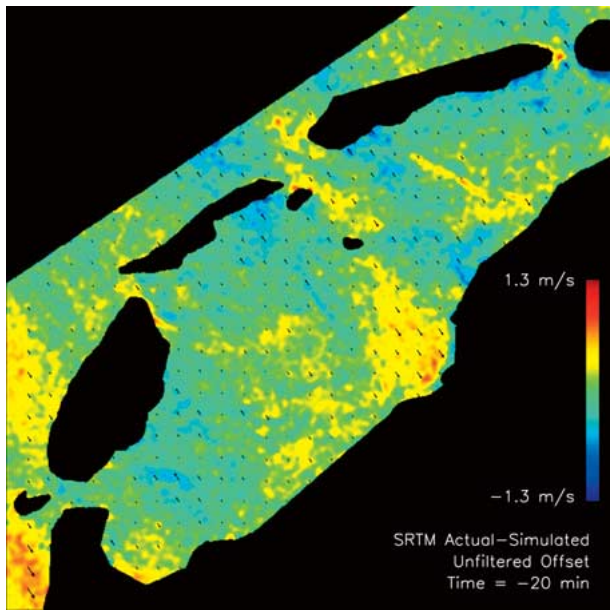

Fig. 12. Difference between the actual and simulated LOS current fields from SRTM (Figs. 3 and 10, respectively).

point was adjusted to be in equilibrium with the local effective wind vector (nominal wind vector minus local surface current vector). Effective wind variations can modulate the magnitude and directional distribution of ocean wave intensities significantly. However, their effect on along-track InSAR signatures is usually small. Further parameters of the simulation are a radar frequency of 9.6 GHz, vertical (VV) polarization, an incidence angle of 55°, and a radar look direction toward $-34°$ from north. For a correct simulation of SAR imaging artifacts (azimuthal displacement of moving targets and blurring) we need the platform altitude (233 km) and velocity (about 7500 m/s) as well as the heading (56°). The simulated along-track InSAR phase and coherence images depend on the effective along-track baseline of 3.5 m. Finally, realistic simulations of statistical properties of the SRTM data require the information that the instrument noise level (noise-equivalent sigma-0) of SRTM is -29 dB and that there are about 64 independent samples of the InSAR phase (effective number of looks) within each grid cell of 100 m $\times$ 100 m. Based on this information, the M4S model converts the surface wave spectrum and LOS current in each grid point into a Doppler spectrum of the backscattered radar signal and generates a realization of a theoretical phase image that is supposed to include all relevant effects and to exhibit the same statistical properties as the actual phase image acquired by SRTM [Fig. 2(b)].

The theoretical SRTM-derived LOS current field obtained from this model result is shown in Fig. 10. It looks very similar to the actual SRTM-derived LOS current field of Fig. 3. However, the scatter plot and the overall statistical quantities shown in Fig. 11 reveal that the simulated SRTM-derived currents agree clearly better with the KUSTWAD-derived currents than the actual SRTM-derived currents, although the distribution of variations on different length scales and other statistical properties of the actual and simulated SRTM-derived currents exhibit quite similar behavior (cf. Fig. 9; diagrams for simulation results not shown explicitly). Of course one must expect some better agreement between the simulated SRTM-derived currents and the KUSTWAD-derived currents due to the fact that the actual surface current field seen by SRTM may have been clearly different from the KUSTWAD current field which has been used as input current field for the simulation *and* as reference current field for the statistical analysis. Further possible sources for a mismatch between simulated and actual SRTM-derived currents are

- residual InSAR processing errors associated with antenna mast oscillation effects;
- errors in the "flat earth" model used to relate the elevations obtained from the conventional cross-track InSAR processing of SRTM data to a horizontal reference plane;
- cross-track InSAR contributions of water level variations within the test area which have not been taken into account in the InSAR simulation;

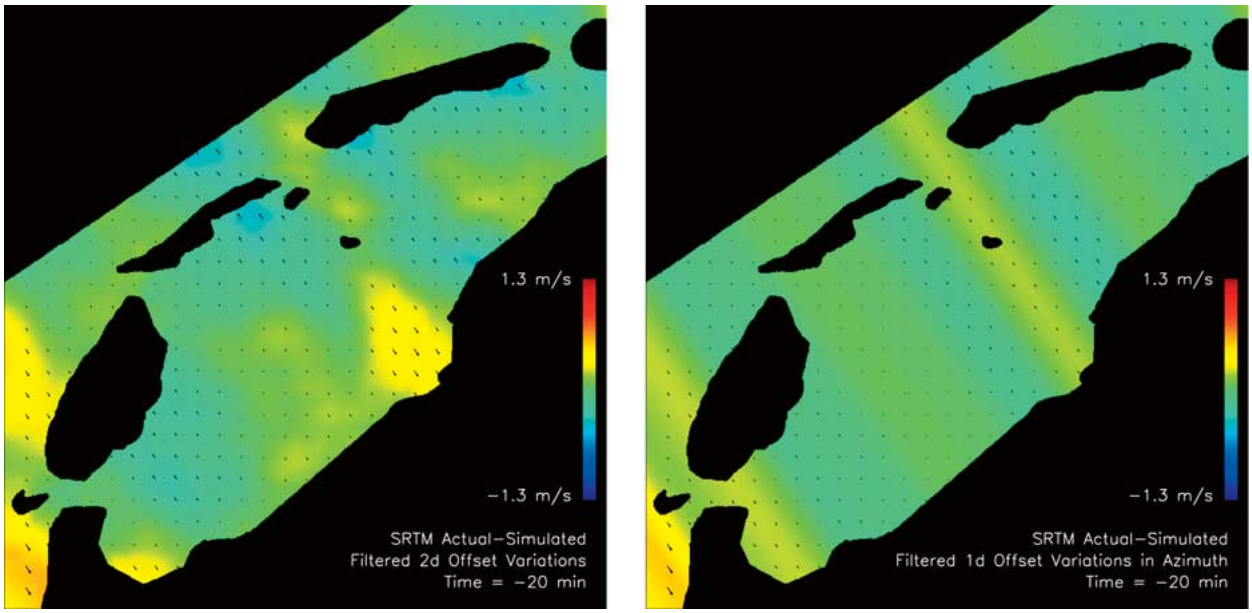

Fig. 13. Low-pass filtered versions of the difference current field of Fig. 12, obtained by (a) applying a 5 km × 5 km running boxcar average filter and (b) averaging in look direction and applying a 5-km running boxcar average filter in flight direction.

- the neglect of wave–current interaction effects in the conversion of the SRTM phase image into a LOS current field and in the simulation;
- a neglect of spatial variations in the wind field and similar effects that may cause inhomogeneities in the surface wave spectrum in the test area;
- other shortcomings of the InSAR imaging model, such as a neglect of nonlinear effects or inadequate parameterizations of some quantities.

Most of these effects should be relatively small on the scales considered here. In principle we could have included corrections for wave–current interaction effects in the data processing and in the simulations, as demonstrated in [4]. Furthermore it is possible to retrieve information on spatial variations in the surface wind field from SAR intensity images, as demonstrated, for example, in [16] and [17]. However, the errors in our SRTM results are dominated by the phase variations associated with antenna mast oscillations, which are already known from other studies [18]. The oscillations result from a specific unexpected problem with the attitude control system of the spacecraft: The failure of a cold gas valve that was intended to stabilize the attitude led to an increased frequency of thruster firings and hence to increased line of sight oscillations of the secondary antenna with amplitudes of several centimeters. These were measured on board with an accuracy of approximately 0.3 mm and later compensated in the SAR processor. The residual error leads to interferometric phase variations on the order of 0.1 rad (equivalent to a horizontal velocity of 0.6 m/s) on typical wavelengths of about 50 km. Another error source are higher frequency oscillations of the mast that were not sampled adequately. Aliasing effects associated with this phenomenon lead to smaller phase oscillations on length scales of a few kilometers.

Fig. 12 shows the spatial distribution of differences between the actual and the simulated SRTM-derived LOS current field in the test area. Aside from small-scale fluctuations, which appear to be dominated by differences between residual phase noise contributions to both current fields, the difference current field exhibits pronounced variations on length scales of 10 km and more. Fig. 13(a) shows a low-pass filtered version of it which was obtained by applying a 5 km × 5 km (51 × 51 grid points) running boxcar average filter. If we subtract this smoothed difference current field from the original SRTM-derived current field of Fig. 3, the correlation with the KUSTWAD-derived currents of Fig. 5(b) improves from 0.558 [see Fig. 6(b)] to 0.858. This shows that the differences between the SRTM-derived LOS current field and the KUSTWAD result for a similar scenario is dominated by variations at wavelengths of 10 km and more. If we modify the SRTM-derived current field by subtracting the array shown in Fig. 13(b), which was obtained by averaging the difference current field of Fig. 12 in look direction and low-pass filtering in flight direction, the correlation with KUSTWAD increases from 0.558 to 0.686. This improvement is less impressive than the improvement with the fully 2-D modification, but it indicates that a considerable portion of the differences between SRTM- and KUSTWAD-derived currents may be associated with the typical phase variations in flight direction that represent residual mast oscillation effects in the SRTM data.

VII. Conclusion and Outlook

Our results show very clearly that the pronounced patterns in the X-band phase image of the western Dutch Wadden Sea from SRTM can be interpreted as signatures of spatial variations in the surface current field. A comparison of the SRTM-derived LOS current field with corresponding current fields from the numerical circulation model KUSTWAD for a full tidal cycle five years before the SRTM mission has shown quite good agreement during a window of about 3 h around the tidal phase corresponding to the SRTM overpass. Correlation coefficients up to 0.6, symmetrical regression coefficients close to 1, mean differences close to 0, and mean rms differences on the order of 0.2 m/s have been found. A further analysis of the current variations on different spatial scales has shown that SRTM is capable of resolving all variations of the LOS current component which

are relevant to the KUSTWAD model, down to spatial scales on the order of 1 km.

Remaining differences between the SRTM-derived LOS currents and the best fit KUSTWAD results are dominated by contributions which vary on length scales of 10 km and more. Such differences may result from shortcomings of the available KUSTWAD model currents due to changes of the bottom topography within five years, inappropriate boundary conditions (e.g., currents, water levels, wind forcing) for the scenario encountered by SRTM, or systematic shortcomings of the model physics, as well as from residual errors in the SRTM data associated with antenna mast oscillations. The latter problems, which really affect the accuracy of the SRTM-derived currents and not just the agreement between SRTM- and KUSTWAD-derived currents, are specific problems of SRTM which can be avoided in future InSAR experiments by using improved antenna metrology techniques. Some further improvement may be obtained by accounting for spatial variations in the surface wave spectrum due to variations in the wind field and for wave–current interaction effects in the algorithm for converting InSAR phases into LOS currents. As shown on earlier occasions and in other contexts, the know-how for correcting along-track InSAR phase images for spatially varying contributions of wave motions [4], [7] as well as for retrieving spatial wind variations from SAR intensity images [16], [17] exists.

Using improved data processing and correction techniques, current retrievals from SRTM and similar spaceborne InSAR configurations could reach an accuracy of about 0.1 m/s rms (instead of 0.24 m/s found between SRTM- and KUSTWAD-derived currents in this exercise) at spatial resolutions on the order of 1 km, which is a quite encouraging result in view of the fact that SRTM was not designed for current measurements at all and had a very limited sensitivity to small LOS velocity variations due to its very short along-track baseline. One can expect significantly better sensitivities, accuracies, and spatial resolutions from dedicated spaceborne along-track InSAR configurations for ocean applications with more favorable system parameters. In contrast to the SRTM configuration, which was a combined along-track/cross-track InSAR, a pure along-track InSAR could also provide absolute current measurements (see [4] for an example) and avoid any problems with current/topography ambiguities, which may be more pronounced in other combined along-track/cross-track InSAR images than in the SRTM image of the Wadden Sea. Furthermore, one can even measure fully 2-D vector current fields during single overpasses if a dual-beam along-track InSAR is used, as recently demonstrated by the University of Massachusetts with a first airborne prototype [19], [20].

We hope that the positive results of this work as well as the promising developments in other recent projects [4], [19], [20] help to promote the idea of using spaceborne along-track InSARs for high-resolution current measurements all over the world and to attract the interests of potential users and operators (space agencies). As a side issue of this work, we have shown once more that the numerical InSAR model of the University of Hamburg, the M4S model, is well suited for realistic simulations of data products of along-track InSARs. This gives us the confidence to use it also for performance evaluations of proposed future InSAR concepts. In a follow-on paper, we will present a study on the current measuring capabilities of the upcoming German satellite TerraSAR-X, which have been found to be surprisingly similar to the capabilities of SRTM.

REFERENCES

[1] R. M. Goldstein and H. A. Zebker, "Interferometric radar measurement of ocean surface currents," *Nature*, vol. 328, pp. 707–709, 1987.

[2] D. R. Thompson and J. R. Jensen, "Synthetic aperture radar interferometry applied to ship-generated waves in the 1989 Loch Linnhe experiment," *J. Geophys. Res.*, vol. 98, pp. 10 259–10 269, 1993.

[3] H. C. Graber, D. R. Thompson, and R. E. Carande, "Ocean surface features and currents measured with synthetic aperture radar interferometry and HF radar," *J. Geophys. Res.*, vol. 101, pp. 25 813–25 832, 1996.

[4] R. Romeiser, "Current measurements by airborne along-track InSAR: Measuring technique and experimental results," *IEEE J. Ocean. Eng.*, 2005, to be published.

[5] D. R. Thompson, "Calculation of microwave Doppler spectra from the ocean surface with a time-dependent composite model," in *Radar Scattering from Modulated Wind Waves*, G. J. Komen and W. A. Oost, Eds. Dordrecht, Netherlands: Kluwer, 1989, pp. 27–40.

[6] R. Romeiser and D. R. Thompson, "Numerical study on the along-track interferometric radar imaging mechanism of oceanic surface currents," *IEEE Trans. Geosci. Remote Sens.*, vol. 38, no. 1, pp. 446–458, Jan. 2000.

[7] R. Romeiser, M. Schwäbisch, J. Schulz-Stellenfleth, D. R. Thompson, R. Siegmund, A. Niedermeier, W. Alpers, and S. Lehner, "Study on concepts for radar interferometry from satellites for ocean (and land) applications (KoRIOLiS). Final Report," Univ. Hamburg, Germany, 2002. [Online]. Available: http://www.ifm.uni-hamburg.de/~romeiser/koriolis.htm.

[8] M. Werner, "Shuttle Radar Topography Mission (SRTM): Mission overview," *J. Telecommun. (Frequenz)*, vol. 55, pp. 75–79, 2001.

[9] L. C. Graham, "Synthetic interferometer radar for topographic mapping," *Proc. IEEE*, vol. 62, no. 6, pp. 763–768, Jun. 1974.

[10] H. Zebker and R. Goldstein, "Topographic mapping from interferometric SAR observations," *J. Geophys. Res.*, vol. 91, pp. 4993–4999, 1986.

[11] B. Rabus, M. Eineder, A. Roth, and R. Bamler, "The Shuttle Radar Topography Mission—A new class of digital elevation models acquired by spaceborne radar," *ISPRS J. Photogramm. Remote Sens.*, vol. 57, pp. 241–262, 2003.

[12] Dutch Hydrographical Service, Tidal heights and streams, coastal waters of The Netherlands and adjacent areas, 2002, Dutch Hydrograph. Service, The Hague, The Netherlands, 2002.

[13] H. H. ten Cate, S. Hummel, and M. R. T. Roest, "An open model system for 2D/3D hydrodynamic simulations," in *Proc. Hydroinformatics 2000*, Madrid, Spain, 2000.

[14] M. E. Philippart and A. W. Gebraad, "Assimilating satellite altimeter data in operational sea level and storm surge forecasting," presented at the *2nd Int. Conf. EuroGOOS*, Southampton, U.K., 2000.

[15] M. Verlaan, "Data assimilation for storm surge forecasting in the North Sea," presented at the *3rd Int. Conf. EuroGOOS*, Southampton, U.K., 2002.

[16] J. Horstmann, W. Koch, S. Lehner, and R. Tomboe, "Wind retrieval over the ocean using synthetic aperture radar with C-band HH polarization," *IEEE Trans. Geosci. Remote Sens.*, vol. 38, no. 5, pp. 2122–2131, Sep. 2000.

[17] F. M. Monaldo, D. R. Thompson, R. C. Beal, W. G. Pichel, and P. Clemente-Colon, "Comparison of SAR-derived wind speed with model predictions and ocean buoy measurements," *IEEE Trans. Geosci. Remote Sens.*, vol. 39, no. 12, pp. 2587–2600, Dec. 2001.

[18] N. Adam, H. Breit, W. Knöpfle, M. Eineder, and S. Suchandt, "The global SRTM X-SAR DEM—Calibration, validation, production stats and results," presented at the *CEOS Working Group on Calibration/Validation SAR Workshop (London, Sep. 2002)*, Noordwijk, The Netherlands, 2003, ESA SP-526.

[19] J. V. Toporkov, M. A. Sletten, D. Perkovic, G. Farquharson, and S. J. Frasier, "Initial vector velocity estimates from the UMass dual beam interferometer," in *Proc. IGARSS*, vol. 2, 2004, pp. 976–979.

[20] D. Perkovic, J. V. Toporkov, M. A. Sletten, G. Farquharson, S. J. Frasier, G. O. Marmorino, and K. P. Judd, "Gulf stream observations obtained with the UMass dual beam interferometer and an infrared camera," in *Proc. IGARSS*, vol. 5, 2004, pp. 3325–3328.

Roland Romeiser (M'00) received the Diplom degree in physics from the University of Bremen, Bremen, Germany, and the Dr.rer.nat. degree from the University of Hamburg, Hamburg, Germany, in 1990 and 1993, respectively.

He is currently a Permanent Staff Scientist at the Institute of Oceanography, University of Hamburg. He has wide experience in the remote sensing of ocean currents, waves, and winds by various microwave sensors. He has been involved in a number of national and international remote sensing projects and experiments. His current research focuses on the theoretical modeling of SAR and InSAR signatures of spatially varying ocean surface currents and the development and evaluation of current retrieval techniques. From August 1998 through July 1999, he spent a year at the Johns Hopkins University, Applied Physics Laboratory as a Feodor Lynen Fellow of the Alexander von Humboldt Foundation.

Dr. Romeiser is an Associate Editor of the IEEE JOURNAL OF OCEANIC ENGINEERING for the topics radar imaging, scatterometry, interferometry, wave–current interaction, and air–sea interaction.

Helko Breit received the Diploma degree in electrical engineering and telecommunication science from the Technical University of Munich, Munich, Germany, in 1990.

In the same year, he joined the German Aerospace Center (DLR), Oberpfaffenhofen, for the development of SAR signal processing algorithms for the SIR-C/X-SAR mission. Later on, he developed the SAR processor for the X-band data of the SRTM mission. He is currently with the Institut für die Methodik der Fernerkundung, Deutsches Zentrum für Luft-und Raumfahrt, Oberpfaffenhofen and is responsible for the development of the TerraSAR-X multimode SAR processor.

Michael Eineder (M'01) received the Diploma degree in electrical engineering and telecommunication science from the Technical University of Munich, Munich, Germany, in 1990, and the Dr.rer.nat. degree from the University of Innsbruck, Innsbruck, Austria, in 2004.

In 1990, he joined the German Aerospace Center (DLR), Oberpfaffenhofen, for the development of SAR signal processing algorithms for the SIR-C/X-SAR mission. Later, he was responsible for the development of the interferometric processing system for SRTM X-SAR. He is currently with the Institut für die Methodik der Fernerkundung, Deutsches Zentrum für Luft-und Raumfahrt, Oberpfaffenhofen, and is leading a team working on algorithms and systems for SAR and interferometric SAR with focus on the future German SAR system TerraSAR.

Hartmut Runge received the diploma in electrical engineering/communications from the University of Siegen, Siegen, Germany, in 1980.

Since that time, he has been a staff member at the German Aerospace Center (DLR), Oberpfaffenhofen, working on various aspects of SAR data processing and applications. He was the Systems Engineer for the Processing and Archiving Facility (PAF) for the X-SAR missions in 1996 and the Project Manager of the X-SAR data processing subsystem for the Shuttle Radar Topography Mission (SRTM) in 2000. Furthermore, he was the Principal Investigator for the SRTM Along Track Interferometry experiments and pioneered the measurement of moving objects like cars and ocean currents from a spaceborne sensor. Fascinated from the great success of the SRTM mission, he has been working for a follow-on mission with a SAR satellite formation flight since the year 2000. For six months, he worked in the Toulouse space center of CNES for the Cartwheel Project and formed a joint DLR/CNES research team. He initiated the implementation of an ATI mode on the TerraSAR-X satellite and is currently the Project Manager of the "TerraSAR-X Traffic Monitoring Project."

Pierre Flament (M'89) received the degree in theoretical physics from the Free University of Brussels, Brussels, Belgium, and the Ph.D. degree in physical oceanography from the Scripps Institution of Oceanography, San Diego, CA, in 1980 and 1986, respectively.

He was a Postdoctoral Fellow at the Woods Hole Oceanographic Institution in 1987–1988, before joining the faculty of the School of Ocean and Earth Sciences and Technology, University of Hawaii, in 1989, where he established a program in ocean remote sensing funded by the National Science Foundation, the National Aeronautics and Space Administartion, and the Office of Naval Research. From 1997 to 2000, he was Scientific Director of the Department of Satellite Oceanography at the French Research Institute for Exploitation of the Sea (IFREMER), Best, in Brest, leading the production of validated scatterometer fields for the World Ocean Circulation Experiment atlas. He was a member of the SIR-C/X-SAR, ERS-2, RADARSAT, and ENVISAT science teams. His research focuses on mesoscale ocean currents and eddies, as observed *in situ*, and remotely by infrared radiometers, scatterometers, SAR, and high-frequency radars.

Karin de Jong, photograph and biography not available at the time of publication.

Jur Vogelzang was born in Amsterdam, The Netherlands, in 1955. He graduated in theoretical physics at the Free University in Amsterdam, and received the Ph.D. degree on his work on modeling bottom signatures in radar images from the University of Utrecht, Utrecht, The Netherlands, in 1981 and 1998, respectively.

After research in theoretical nuclear physics at the same university, he joined Rijkswaterstaat, Delft, The Netherlands, in 1987. There, he worked in various departments on development and implementation of new measurement techniques based on remote sensing. He has been involved in a large number of national and international remote sensing projects and experiments. He is specialized in microwave remote sensing. Since 2005, he has been working at the Royal Netherlands Meteorological Institute (KNMI) as a Researcher in the field of wind scatterometry.